# Jupiter, the great celestial organizer: On the origin of orbits of some asteroid families in mean motion resonances with Jupiter

Judit Slíz-Balogh [a,b,c], Dániel Horváth [b], Gábor Horváth [b,c,*]

[a] Department of Astronomy, ELTE Eötvös Loránd University, H-1117, Budapest, Pázmány sétány 1, Hungary
[b] Environmental Optics Laboratory, Department of Biological Physics, ELTE Eötvös Loránd University, H-1117, Budapest, Pázmány sétány 1, Hungary
[c] Astropolarimetry Research Group, Office of Supported Research Groups, Eötvös Loránd Research Network, H-1052, Budapest, Piarista utca 4, Hungary

ABSTRACT

The mechanism that forms the different resonant families of the asteroid belt between the orbits of Jupiter and Mars is not completely understood. To study the resonant capture mechanism and the origin of orbits of some asteroid families in mean motion resonances with Jupiter, furthermore to give a possible explanation of this problem, we performed *in situ* numerical simulations of the 3-dimensional semi-analytical model of the Sun-Jupiter-particle system. We examined the numbers and orbits of particles captured along the Jupiter's present orbit (including the L3, L4 and L5 Lagrange points) for 7000 Jupiter years. In our simulations we did not distinguish between planetesimals, interplanetary dust and asteroids, because we investigated the restricted three-body problem taking into account only gravitation. We found that the asteroid families in 4:3, 1:1, 4:5, 3:4, 2:3, 5:8, 4:7 and 5:9 resonances may have formed from the asteroids captured, launched and kept on their orbits not only by the L4 and L5 points, but also by the unstable L3 point and certain areas along the Jupiter's path. Furthermore, we found possible new asteroid families in 4:5 and 3:4 resonances, no any member of which have yet been identified. Thus, Jupiter forms a shield which protects the inner Solar System from asteroids moving with speeds not significantly differing from that of Jupiter.

## 1. Introduction

Since 1801, when Giuseppe Piazzi discovered the first asteroid, Ceres, the origin, characteristics, behaviour and evolution of asteroids in the Solar System receive much attention. Here first, we give a brief overview of some relevant works investigating the Jupiter's resonant asteroid families, then we review the most frequently studied asteroids, the Trojans and Greeks formed around the L4 and L5 Lagrange points of Sun and the giant planets, finally we explain the motivation and aim of our present study.

Using numerical simulations, [1] investigated the chaotic motion of asteroids having nearly 12:7 mean motion resonance with Jupiter. They studied also the escape of these asteroids, and found stable chaos due to the stickiness effect, thus there are no periodic orbits corresponding to this resonance. [2] showed that resonant periodic orbits also lack in other high-order (11:4, 13:6, 18:7, 22:9) resonances with Jupiter, and such asteroids with stable-chaotic orbits have really been observed. [3] investigated the chaotic behaviour of Jupiter's Trojan asteroids. They

integrated a set of fictitious objects and numbered Trojans for $10^9$ Earth years with a time step of 0.1 Earth year. They found that 17% of the numbered Trojans are unstable over the age of the Solar System, and the instability is the result of chaotic diffusion.

[4] showed with numerical simulations that the Hilda asteroids in the 3:2 mean motion resonance with Jupiter are very stable. However, if these asteroids escape, then their perihelion distances p are greater than 2.5 AU (= Astronomical Unit), that is the number of escaped Hildas reaching the inner Solar System (p < 2.5 AU) is negligible.

[5] studied the motion of 9200 test particles around Jupiter and Saturn while the latter crossed the 2:1 resonance. They found that this crossing has a great influence on the orbits of both the asteroids and the moons. Presumably, most of the irregular moon's orbits were generated during the 2:1 resonance crossing.

[6] investigated the evolution and stability of asteroids in 2:1, 3:2, 4:3 first order mean motion resonances with Jupiter. They found that the primordial asteroids in the J3:2 resonance were effectively removed from their orbits when Jupiter and Saturn crossed their 2:1 resonance.

**Fig. 1.** Out-of-scale schematic drawing of the elliptical orbit of Jupiter (with excentricity e = 0.048) around the center of mass C of the Sun-Jupiter system and the five Lagrange points L1, L2, L3, L4 and L5 in the Jupiter's orbital plane. L4 and L5 are at the vertices of two equilateral triangles formed by Sun (S), Jupiter and L4/L5. L4 leads Jupiter, while L5 follows it. The Greek and Trojan asteroids librate around the L4 and L5 point, respectively. The origin O of the x-y system of coordinates coincides with C. Axis z is perpendicular to the Jupiter's orbital plane.

[7] modelled the long-term evolution of the collisional subgroup of the Hilda family located in the 3:2 mean motion resonance with Jupiter. They found that the current collisional activity of these asteroids is very low. They concluded that probably this subgroup might have been formed during the Late Heavy Bombardment when the collisions were much more frequent.

[8] studied with numerical methods third and fourth order mean motion resonances of the restricted three-body problem for mass ratios approximately corresponding to those of the Sun-Jupiter and Sun-Neptune systems. They found that there are different regions of librations within each resonance.

Applying long-term (≤100 Myr) numerical integrations, [9] demonstrated the possibility of asteroids coming from the Hungaria family being captured by the terrestrial planets of the inner Solar System into co-orbital motion. They concluded that the Hungaria region is a source of objects co-orbiting with Mars and Earth.

Let us consider the Trojan and Greek asteroids of Sun and the giant planets: [10] investigated the long-term motion of the Trojans around the L4 and L5 Lagrange points of the Sun-Jupiter system. They searched for asteroidal families among the Trojans and found two families around L4, but no one around L5. [11] found that the Trojans could be split up into four different resonance families, and then they generalized these families [12].

[13] studied how the stability of the Jovian Trojans is influenced by the resonant configurations of the outer planets, especially Jupiter and Saturn. They showed that the 2S:1J and 5S:2J Saturn:Jupiter resonances cause the greatest instability among the Jovian Trojans, while other resonances (e.g. 7S:3J) are less disruptive.

[14] investigated the behaviour of particles in the vicinity of the L4 and L5 points of Jupiter, Saturn, Uranus and Neptune. They found that the present population of Trojans is probably different in both the trajectory and size distribution from the primordial population.

[15] investigated the dynamics of Jovian Trojans when Jupiter was in 2:1 mean motion resonance with Saturn. When Jupiter and Saturn approach, reach and leave this resonance, the Jovian Trojan orbits considerably change.

[16] studied the stable region around the Lagrange point L4 in the elliptic restricted three-body problem. The size of such regions are minimal where there are resonances between the libration frequencies of motions around L4.

On the basis of the Floquet's theory, [17] investigated the stability of the L4 point in the elliptic restricted three-body problem, and determined the stable and unstable regions around L4 as functions of the mass ratio and eccentricity.

[18] studied the secondary resonances and the stability of the L4 point in the spatial restricted three-body problem for mass ratios $\mu = m_{small}/(m_{small} + m_{large}) \leq 0.0045$.

Using hydro-simulations of the evolution of a protoplanetary disk, [19] found that the size distribution of captured particles ranging from μm-cm (Trojan dust particles) to km (rocks, Trojan asteroids) is different between the L4 and L5 Lagrange points.

In spite of the above-mentioned thorough investigations, the mechanism that forms the different resonant families of the asteroid belt between the orbits of Jupiter and Mars is not yet well understood. Therefore, in this work we study the co-orbital motion of numerous dynamically cold particles (asteroids) with negligible mass confronting Jupiter's path, under the sole gravitational influence of Sun and Jupiter. Jupiter arranges the not-escaped particles into different resonance families, the further fate of which may be influenced by such factors as planet migration [20], Yarkovsky effect, that is the force acting on a rotating body caused by the anisotropic heat emission [21] and collisions [7], for example. [22] investigated the influence of the Yarkovsky force on the long-term orbital evolution of Jupiter Trojan asteroids. They found that objects with radii R < 1 km are significantly influenced by the Yarkovsky force, therefore it is essential to take it into account for the long-term (Myr, Gyr) studies of asteroids. In our simulations we examined the motion of particles in the relatively short (80 000 year) period after their capture. On the other hand, we also showed that the gravitational force of the Sun-Jupiter system alone is sufficient enough for the formation of resonant asteroid families, the trajectories of which may be later perturbed by the Yarkovsky effect, for example, but the latter effect was not studied.

Here we focuse to the problem, how Sun and Jupiter, with their present parameters (orbits and masses), can capture in situ particles (either from planetesimal or debris disk, or resonant interplanetary dust or asteroid ring), into different resonant families from a dynamically cold particle swarm with which it meets along its presents orbit including the L3, L4 and L5 Lagrange points. This approach means a discontinuous sampling from a continuous particle disk along the Jupiter's orbit. We took 7 probes from this disk and studied the formation of the 4:3, 1:1, 4:5, 3:4, 2:3, 5:8, 4:7 and 5:9. resonant families.
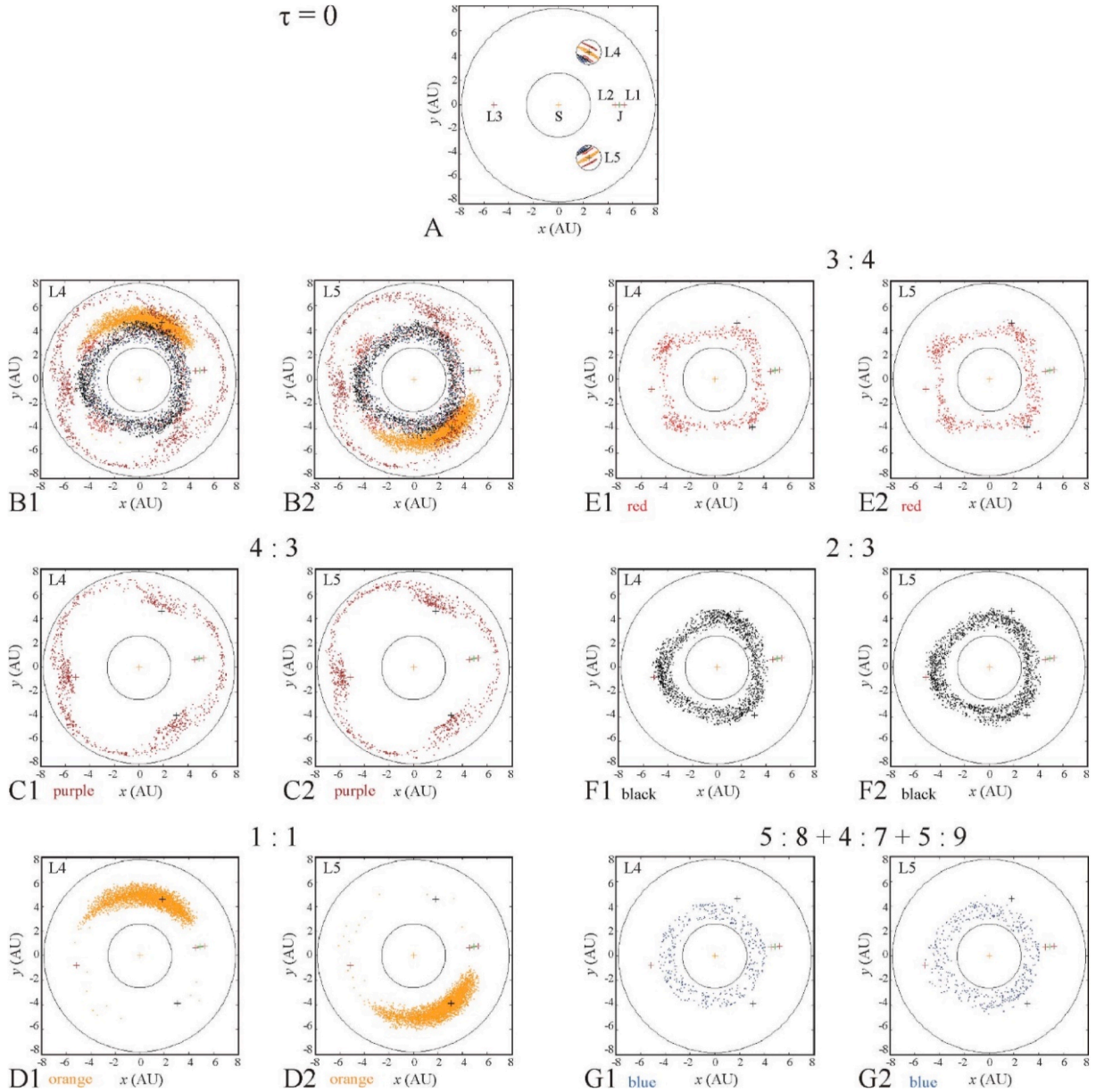
**Fig. 2.** x-y projections of the initial (A) and final (B–G) positions of trapped particles of the spherical initial domain (SID) centred around the L4 and L5 Lagrange points for $\tau = 0$ Earth day, where $\tau$ is the time of Jupiter's pericenter passage. The differently coloured dots depict particles in different n:m mean motion resonances with Jupiter (while Jupiter completes n orbits, the particle runs m ones around Sun) as follows: purple 4:3 (C1, C2), orange 1:1 (D1, D2), red 3:4 (E1, E2), black 2:3 (F1, F2), blue 5:8, 4:7 and 5:9 (G1, G2). The two big circles indicate the boundaries of the spherical shell (SS). (A) Initial coordinates of all trapped particles. The two small circles centred at L4 and L5 indicate the two SIDs. (B1, B2) Positions of all trapped particles started from the SID centred around L4 and L5 after 7000 Jupiter years. (C1, C2) As B1, B2 for trapped particles started from the purple (4:3) zone of the SIDs. (D1, D2) As C1, C2 for the orange (1:1) zone of SIDs. (E1, E2) As C1, C2 for the red (3:4) zone of SIDs. (F1, F2) As C1, C2 for the black (2:3) zone of SIDs. (G1, G2) As C1, C2 for the blue (5:8 + 4:7 + 5:9) zones of SIDs (see also Supplementary Stereo Cube C1 and Supplementary Video Clips VC7-VC9, VC11-VC16). (For interpretation of the references to colour in this figure legend, the reader is referred to the Web version of this article.)

## 2. Model and methods

We used a 3-dimensional semi-analytical model of the Sun-Jupiter-particle system taking into account only the gravitational effects of Sun and Jupiter, where the particle has a negligible mass relative to the two primaries. Both Jupiter and Sun have elliptical orbits with excentricity e = 0.048 around their center of mass C in the same plane (Fig. 1). The elliptical motion of Jupiter around C was calculated with the well-known formalism of the two-body problem. Taking into account the gravitation of Sun and Jupiter, the motion of a particle (asteroid) with mass $m_p$ starting from the vicinity of the L4 or L5 Lagrange point of the Sun-Jupiter system was described by the equation of motion in the C-xyz

system of coordinates (Fig. 1):

$$m_p \ddot{x}_p = -\frac{\partial U}{\partial x_p}, \quad m_p \ddot{y}_p = -\frac{\partial U}{\partial y_p}, \quad m_p \ddot{z}_p = -\frac{\partial U}{\partial z_p}, \tag{1}$$

$$U = -G \sum_{j=1}^{j=2} \frac{m_p m_j}{r_{pj}}, \tag{2}$$

$$r_{pj} = \sqrt{(x_p - x_j)^2 + (y_p - y_j)^2 + (z_p - z_j)^2},$$
$$j = 1, 2,$$

where $x_p$, $y_p$ and $z_p$ are the Descartes coordinates of the particle, j = 1

**Table 1**
Initial coordinates $x_0$, $y_0$, $z_0$ (AU) of Sun, Jupiter and the L4 and L5 Lagrange points in the C-xyz coordinate system for $\tau = 0$, 1084, 2168, 3252 Earth days (Ed), where $\tau$ is the time of Jupiter's pericenter passage.

|  |  | $\tau = 0$ Ed | $\tau = 1084$ Ed | $\tau = 2168$ Ed | $\tau = 3252$ Ed |
|---|---|---|---|---|---|
| Sun | $x_0$(AU) | −0.004722 | 0.000484 | 0.005202 | 0.000469 |
|  | $y_0$(AU) | 0.000000 | −0.004950 | 0.000007 | 0.004951 |
|  | $z_0$(AU) | 0.000000 | 0.00000 | 0.000000 | 0.000000 |
| Jupiter | $x_0$(AU) | 4.946837 | −0.506693 | −5.44996 | −0.491454 |
|  | $y_0$(AU) | 0.000000 | 5.186053 | −0.007566 | −5.186779 |
|  | $z_0$(AU) | 0.000000 | 0.000000 | 0.000000 | 0.000000 |
| L4 | $x_0$(AU) | 2.471057 | −4.748646 | −2.715820 | 4.250678 |
|  | $y_0$(AU) | 4.288175 | 2.151323 | −4.728088 | −3.016932 |
|  | $z_0$(AU) | 0.000000 | 0.000000 | 0.000000 | 0.000000 |
| L5 | $x_0$(AU) | 2.471057 | 4.242436 | −2.728937 | −4.741662 |
|  | $y_0$(AU) | −4.288175 | 3.029780 | 4.720530 | −2.164896 |
|  | $z_0$(AU) | 0.000000 | 0.000000 | 0.000000 | 0.000000 |

and 2 refers to Sun and Jupiter (main bodies), respectively, U is the particle's potential energy, G is the gravitational constant, $m_j$ is the mass of main bodies, and $r_{pj}$ is the distance between the particle and the j-th mass. We converted (1) to a system of first order differential equations that was numerically integrated by a Runge-Kutta-Fehlberg 7(8) integrator [23] with an adaptive step size determined by an accuracy of $10^{-21}$ with a starting time step of 4 Earth days. In these calculations, the length and time units were the astronomical unit (AU) and the orbital period of Jupiter (1 Jupiter year = 4333.2867 Earth days), respectively. Our computer simulations were calculated at the ELTE HPC 2019 supercomputer of the Eötvös Loránd University (Budapest, Hungary).

A particle was considered as trapped, if it remained in a spherical shell (SS) with origin at the center of mass C of the Sun-Jupiter system for 7000 Jupiter years with minimum and maximum radii $r_{min} = 0.5r_0 \leq r \leq r_{max} = 1.5r_0$, where $r_0 = 5.1984$ AU is the semi-major axis of the Jupiter's orbit around C. On the other hand, a particle was considered as escaped, if it left the SS within 7000 Jupiter years, or entered the sphere of influence (SOI) of Jupiter with radius $r_{SOI} = 48200000$ km.

First, we considered 69420 equidistant points which fall into the sphere with 2 AU diameter inscribed in this cube. The cloud of these points are called spherical initial domain (SID) further on this work. They are the "probes" mentioned in the Introduction. This SID was centred around the L4 and L5 points, or around other points along the Jupiter's orbit further away from L4 and L5. For both L4 and L5 there were 4 SIDs along the Jupiter's orbit with starting points of time $\tau = 0$, 1084, 2168 and 3252 Earth days, where $\tau$ is the time of Jupiter's pericenter passage (Fig. 2, Table 1). From the mentioned points of the SID we launched 69420 particles, the initial linear velocity vector of which was equal to that of L4/L5, that is their initial velocity component perpendicular to the Jupiter's orbital plane was zero.

The approximate coordinates of the collinear Lagrange points L1, L2 and L3 were calculated on the basis of the data in Appendices I–III of [24] as follows: the average distances of the L1 and L2 points from Jupiter are 0.363 and 0.347 AU, respectively, while the average distance of the L3 point from Sun is 5.2 AU.

## 3. Results

Fig. 2 (see also Supplementary Stereo Cube C1) illustrates the initial and final positions of the trapped particles (asteroids) started from the SID around the L4 and L5 points for $\tau = 0$ Earth day. Fig. 2A shows the initial positions of trapped particles which compose 5 sharply separated zones (bands, marked with different colours) divided by empty gaps. The particles belonging to a given zone have the common property that they are in the same n:m mean motion resonance with Jupiter, that is, while Jupiter completes n orbits, the particle runs m ones around Sun. Fig. 2B1 and 2B2 depict the differently coloured positions of all trapped particles with different n:m resonances after 7000 Jupiter years.

Fig. 2C1 and 2C2 display the final positions of trapped particles outside the Jupiter's orbit in 4:3 resonance. These particles are dispersed along a Sun-centred trifolium-shaped torus with three remarkable condensation clouds at the Lagrange points L3, L4 and L5. They may correspond to the Thule asteroids, 7 members of which are currently known. According to the number of simulated particles (Table 2), they can be much numerous than seven. Thus, it would be worth searching for further Thule members. Fig. 2D1 and 2D2 show the final positions of trapped particles in 1:1 resonance along the Jupiter's orbit. These crescent-shaped particle clouds correspond to the Greek and Trojan asteroids of Jupiter centred around L4 and L5, respectively.

Fig. 2E1 and 2E2 represent the final positions of trapped particles in 3:4 resonance inside the Jupiter's orbit. These particles disperse along a quadratic torus centred at Sun with four clear condensation clouds. No any member of the 3:4 asteroid family have been identified yet.
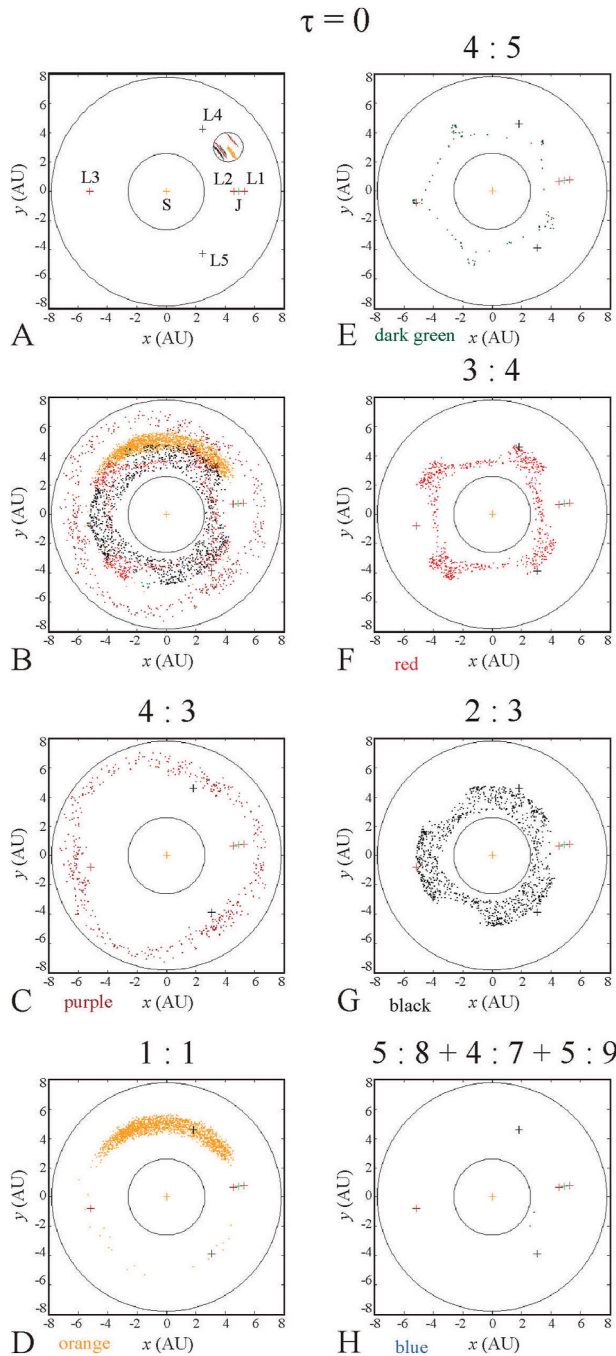
Fig. 2F1 and 2F2 show the final positions of trapped particles in 2:3 resonance inside the Jupiter's orbit. These particles are scattered along a Sun-centred triangular torus, at the apexes of which condensation clouds form around the L3, L4 and L5 Lagrange points. Based on the location and resonance of these particles, they may belong to the Hilda family, which has about 5000 known members.

The shape of particle zones in 5:8, 4:7 and 5:9 (3rd and 4th order) resonances (Fig. 2G1, 2G2) is a Sun-centred circular torus. They may correspond to subgroups of the outer main asteroid belt.

Supplementary Fig. S1 displays the same as Fig. 2, but for $\tau = 1084$ Earth days. Further on we write only about the differences between Fig. 2 and the actual figure. While in Supplementary Fig. S1C1 the trifolium-shaped torus has dense particle clouds around the L3, L4 and L5 points, such condensations do not exist in Fig. S1C2. Although in Figs. S1E1 and S1E2 the quadratic particle torus around Sun is visible, there are no particle clouds in Fig. S1E1, while the quadratic torus in Fig. S1E2 contains again four condensation clouds. In Figs. S1F1 and S1F2 numerous particles are gathered again along a triangular torus. Supplementary Figure S1G1 contains many particles, but in Fig. S1G2 there are only a few particles.

Supplementary Figure S2 depicts the same as Fig. 2 for $\tau = 2168$ Earth days. Both Figs. S2C1 and S2C2 display practically the same trifolium-shaped particle torus without particle condensation around the L3, L4 and L5 points. In Figs. S2G1 and S2G2 there are only very few particles.

Supplementary Fig. S3 shows the same as Fig. 2 for $\tau = 3252$ Earth days. In Figs. S3C1 and S3C2 the trifolium-shaped torus is also present,

**Table 2**
Number of captured particles (trapped from the original 69420 particles) of the zones in 4:3, 1:1, 3:4, 2:3, 5:8 + 4:7 + 5:9 resonances in the spherical initial domain (SID), the center of which coincides with the Lagrange points L4($\tau$) and L5($\tau$) of the Sun-Jupiter system for different time $\tau$ (Earth day) of Jupiter's pericenter passage. The colours in the brackets correspond with those of the particles in different mean motion resonances in Fig. 2 (see also Supplementary Figs. S1–S3).

| resonance zone | L4 ($\tau = 0$) | L5 ($\tau = 0$) | L4 ($\tau = 1084$) | L5 ($\tau = 1084$) | L4 ($\tau = 2168$) | L5 ($\tau = 2168$) | L4 ($\tau = 3252$) | L5 ($\tau = 3252$) |
|---|---|---|---|---|---|---|---|---|
| 4:3 (Thule, purple) | 1854 | 1854 | 2216 | 2152 | 2100 | 2114 | 2126 | 2225 |
| 1:1 (Trojan, orange) | 9007 | 9014 | 10070 | 10002 | 11170 | 11179 | 10023 | 10053 |
| 3:4 (red) | 1064 | 1214 | 704 | 732 | 216 | 211 | 738 | 701 |
| 2:3 (Hilda, black) | 2887 | 2828 | 2673 | 2255 | 2441 | 2444 | 2246 | 2373 |
| 5:8 + 4:7 + 5:9 (blue) | 583 | 500 | 1359 | 5 | 8 | 2 | 0 | 1661 |
| sum | 15395 | 15410 | 17022 | 15146 | 15935 | 15950 | 15133 | 17013 |

**Fig. 3.** Same as Fig. 2, but the SID's center is the L5 point for $\tau = 1084$ Earth days, while Sun and Jupiter are in their initial position corresponding to $\tau = 0$ Earth day. (A) Initial coordinates of all trapped particles. The smallest circle indicates the SID. (B) Positions of all trapped particles started from the SID after 7000 Jupiter years. (C) As B for trapped particles started from the SID's purple (4:3) zone. (D) As C for the SID's orange (1:1) zone. (E) As C for the SID's dark-green (4:5) zone. (F) As C for the SID's red (3:4) zone. (G) As C for the SID's black (2:3) zone. (H) As C for the SID's blue (5:8 + 4:7 + 5:9) zones. (For interpretation of the references to colour in this figure legend, the reader is referred to the Web version of this article.)

and the particle clouds around the L3, L4 and L5 points are denser in Fig. S3C2 than in Fig. S3C1. In Figs. S3F1 and S3F2 the particles are dispersed along a triangular torus, but the three particle clouds around the L3, L4 and L5 points are denser in Fig. S3F1 than in Fig. S3F2. In Fig. S3G1 there are no particles, while in Fig. S3G2 the particles form a circular torus.
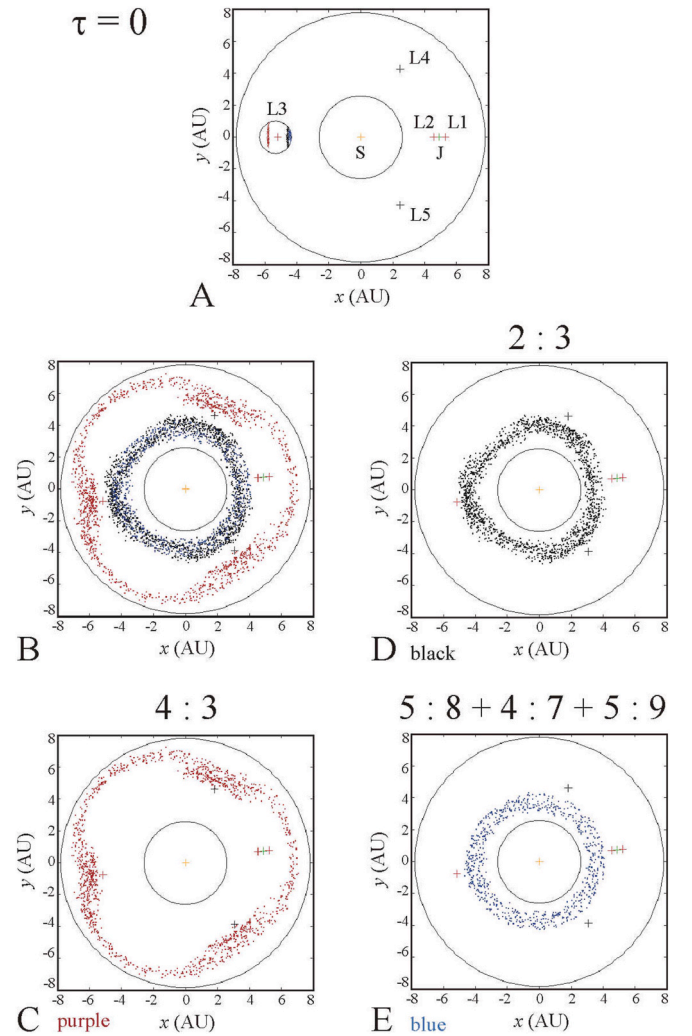


**Fig. 4.** Same as Fig. 3, but the SID's center is the L3 point belonging to $\tau = 0$ Earth day. (A) Initial coordinates of all trapped particles. The smallest circle centred at the L3 point indicates the SID. (B) Positions of all trapped particles started from the SID after 7000 Jupiter years. (C) As B for trapped particles started from the SID's purple (4:3) zone. (D) As C for the SID's black (2:3) zone. (E) As C for the SID's blue (5:8 + 4:7 + 5:9) zones. (For interpretation of the references to colour in this figure legend, the reader is referred to the Web version of this article.)

We also investigated how many particles along the Jupiter's orbit contribute to the formation of resonance families at locations other than the L4 and L5 Lagrange points. These results are shown in Figs. 3 and 4, Supplementary Figs. S4–S6 and Table 3. Among the particles trapped between the L4/L5 points and Jupiter at $\tau = 0$, a pentagon-shaped new resonance group appears, namely the 4:5 resonance. We found that far from the L4 and L5 points, approximately 33% of particles captured by L4/L5 are trapped (Table 3).

Fig. 3 displays the trapped particles when the SID's center is the L5 point belonging to $\tau = 1084$ Earth days, while Sun and Jupiter are in their initial position corresponding to $\tau = 0$ Earth day. In Fig. 3 a pentagon-shaped new resonance group occurs, namely the 4:5 resonance. Practically, there are no particles in 5:8, 4:7 and 5:9 resonances, while other results/details are qualitatively the same as in Supplementary Fig. S1 for L5.

Supplementary Fig. S4 shows the trapped particles when the SID's center is the L4 point belonging to $\tau = 1084$ Earth days, while Sun and Jupiter are in their initial position corresponding to $\tau = 0$ Earth day. In Fig. S4 practically there are no particles in 4:3 and 1:1 resonances, while

**Table 3**

Number of trapped particles of the zones in 4:3, 1:1, 4:5, 3:4, 2:3, 5:8, 4:7 and 5:9 resonances in the spherical initial domain (SID) of Figs. 3 and 4 and Supplementary Figs. S4–S6 where Sun and Jupiter are in their initial position at τ = 0 Earth day. The center of the SID coincides with the Lagrange points L3(τ), L4 (τ) and L5(τ) of the Sun-Jupiter system for different time τ (Earth day) of Jupiter's pericenter passage. The colours in the brackets correspond with those of particles in different mean motion resonances in Figs. 3 and 4 and Supplementary Figs. S4–S6.

| Sun and Jupiter in their initial position at τ = 0 | | | | |
|---|---|---|---|---|
| **SID's center at** | | | | |
| resonance zone | L5(τ = 1084) | L4(τ = 1084) | L3(τ = 0) | L4(τ = 2168) | L4(τ = 3252) |
| 4:3 (Thule, purple) | 850 | 0 | 2464 | 0 | 838 |
| 1:1 (Trojan, orange) | 2987 | 46 | 0 | 2733 | 2930 |
| 4:5 (dark green) | 163 | 0 | 0 | 0 | 171 |
| 3:4 (red) | 1060 | 794 | 0 | 291 | 1034 |
| 2:3 (Hilda, black) | 1656 | 1982 | 2811 | 0 | 1615 |
| 5:8 + 4:7 + 5:9 (blue) | 4 | 1986 | 1109 | 105 | 3 |
| Sum | 6720 | 4808 | 6384 | 3129 | 6592 |

other results/details are qualitatively the same as in Supplementary Fig. S1 for L4.

Fig. 4 represents the trapped particles when the SID's center is the L3 point belonging to τ = 0 Earth day. In Fig. 4 the 1:1 and 3:4 resonance families are missing, however, the 4:3, 3:2 and 5:8 + 4:7 + 5:9 families appear prominently.

Supplementary Fig. S5 displays the trapped particles when the SID's center is the L4 point belonging to τ = 2168 Earth days, while Sun and Jupiter are in their initial position corresponding to τ = 0 Earth day. In Fig. S5 there are very few particles, and practically there are only particles in the 1:1 and 3:4 resonances.

Supplementary Fig. S6 shows the trapped particles when the SID's center is the L4 point belonging to τ = 3252 Earth days, while Sun and Jupiter are in their initial position corresponding to τ = 0 Earth day. In Fig. S6 (similarly to Fig. 3) a pentagon-shaped new resonance group appears, namely the 4:5 resonance. Practically, there are no particles in 5:8, 4:7 and 5:9 resonances, while other results/details are qualitatively the same as in Supplementary Fig. S3 for L4.

Fig. 5 represents some typical trajectories of particles (asteroids) in the 4:3, 1:1, 4:5, 3:4 and 2:3 (first-order) resonances with Jupiter (see also Supplementary Video Clips VC1-VC6). In Fig. 5A there are three inner loops near the L3, L4 and L5 Lagrange points during one revolution of the particle in 4:3 resonance with Jupiter, which is characteristic of the Thule-family. The particle starts from nearby the L4 point. Fig. 5B displays tadpole orbits of particles around L4 and L5 after 50 revolutions. Fig. 5C shows a horseshou orbit after 200 revolutions. In Fig. 5D the particle's orbit is a regular pentangle with five small loops at the vertices. One of the vertices is near L3. In Fig. 5E one can see a regular quadrangle with four loops at its corners. The orbit starts from nearby the L4 point, while the other three vertices are far from the Lagrange points. Fig. 5F represents an equilateral triangle-shaped orbit, which is characteristic of the Hilda-family.

## 4. Discussion and conclusions

Due to the nature of the Jupiter's elliptical orbit, there are significant differences in the capture efficiency of the two stable Lagrange points L4 and L5 at different orbital sites (i.e., at different time τ of Jupiter's pericenter passage). The largest differences in the number of simulated Trojan and Thule asteroids are between the Jupiter's perihelion (τ = 0 Earth day) and aphelion (τ = 2168 Earth days). The number of simulated Trojan and Greek asteroids (1:1 resonance, orange zone in

Figs. 2–4 and Supplementary Figs. S1–S6) captured at τ = 2168 Earth days is larger by 24% than that trapped at τ = 0 Earth day. The number of simulated Thule asteroids (4:3 resonance, purple zone in Figs. 2–4 and Supplementary Figs. S1–S6) trapped at τ = 2168 Earth days are greater by 13% than that captured at τ = 0 Earth day. In the contrary, for the 3:4 (red in Figs. 2–4 and Supplementary Figs. S1–S6) and 2:3 (black, Hilda in Figs. 2–4 and Supplementary Figs. S1–S6) resonances the number of simulated asteroids captured near the perihelion is larger than that trapped near the aphelion. In the case of 5:8, 4:7 and 5:9 (blue in Figs. 2–4 and Supplementary Figs. S1–S6) third and fourth order resonances, the most simulated asteroids are captured by the L4 point at τ = 1084 Earth days and by the L5 point at τ = 3252 Earth days (Table 2).

In our model, we placed the SID containing the 69420 particles near the L4 and L5 points, because we wanted to study their capture into the 1:1 resonance. We found that the initial positions of captured particles compose 5 sharply separated zones divided by empty gaps (Fig. 2A and Supplementary Figs. S1A, S2A, S3A). However, the trapped particles surprisingly formed not only the 1:1 resonance families (i.e., Trojans and Greeks), but also the 4:3, 4:5, 3:4, 2:3, 5:8, 4:7, 5:9 families.

Each resonance family is supplemented with asteroids trapped by certain points along the Jupiter's orbit, not necessarily by the L4 and L5 Lagrange points. On the basis of the results presented in this work, we propose that not only the 1:1, but also the 4:3, 4:5, 3:4, 2:3, 5:8, 4:7 and 5:9 resonance families may originate from the Jupiter's orbit, mainly, but not only, due to the influence of the L3, L4 and L5 Lagrange points. Since the Lagrange points L4 and L5 cannot capture high-speed particles, in our simulations we chose the same initial speed of all particles as those of the L4 and L5 points. We investigated only the particle capture, rather than their subsequent migration. We have seen that the efficiency of particle capture is not uniform along the Jupiter's orbit. Since there is no information about the distribution of particles along this orbit, as a first approximation we assumed a uniform distribution in our simulations. On the basis of Fig. 2, Supplementary Figs. S1–S3 and Table 2 we conclude the following:

- In case of τ = 0 Earth day, the most trapped particles are in 3:4 and 2:3 resonances, and the fewest captured particles occur in 4:3 and 1:1 resonances with Jupiter compared to other starting values of Jupiter's pericenter passage τ, while the number of particles captured by the L4 and L5 Lagrange points is practically the same.
- For τ = 1084 Earth days, the number of particles captured by L4 and L5 is the same except the 5:8, 4:7 and 5:9 third and fourth order resonances, where L4 captures many (1359) particles, while L5 almost none (5).
- For τ = 2168 Earth days, the L4 and L5 points capture the most particles compared to other τ-values, and the number of particles trapped by L4 and L5 is approximately the same.
- For τ = 3252 Earth days, the number of particles captured by L4 and L5 is the same except for the 5:8, 4:7 and 5:9 (third and fourth order) resonances, where L5 captures many (1661) particles, while L4 none.

Based on Figs. 3 and 4, Supplementary Figs. S4–S6 and Table 3, when Sun and Jupiter are in their initial position at τ = 0 Earth day, and the SID's centers correspond with the L4 and L5 points belonging to other τ-values, we conclude the following:

- Significantly fewer particles are trapped along the Jupiter's orbit far from the L4 and L5 points than around both points.
- The 4:5 new resonance family appears in case of SID's centers at L5(τ = 1084 Earth days) and L4(τ = 3252 Earth days).
- In case of SID's center at L3(τ = 0 Earth day), there are particles only in the 4:3 (Thule), 2:3 (Hilda) resonances and the 5:8, 4:7 and 5:9 third and fourth order resonances.

Considering the asteroid families of Jupiter, our conclusions are:

$$\tau = 0$$
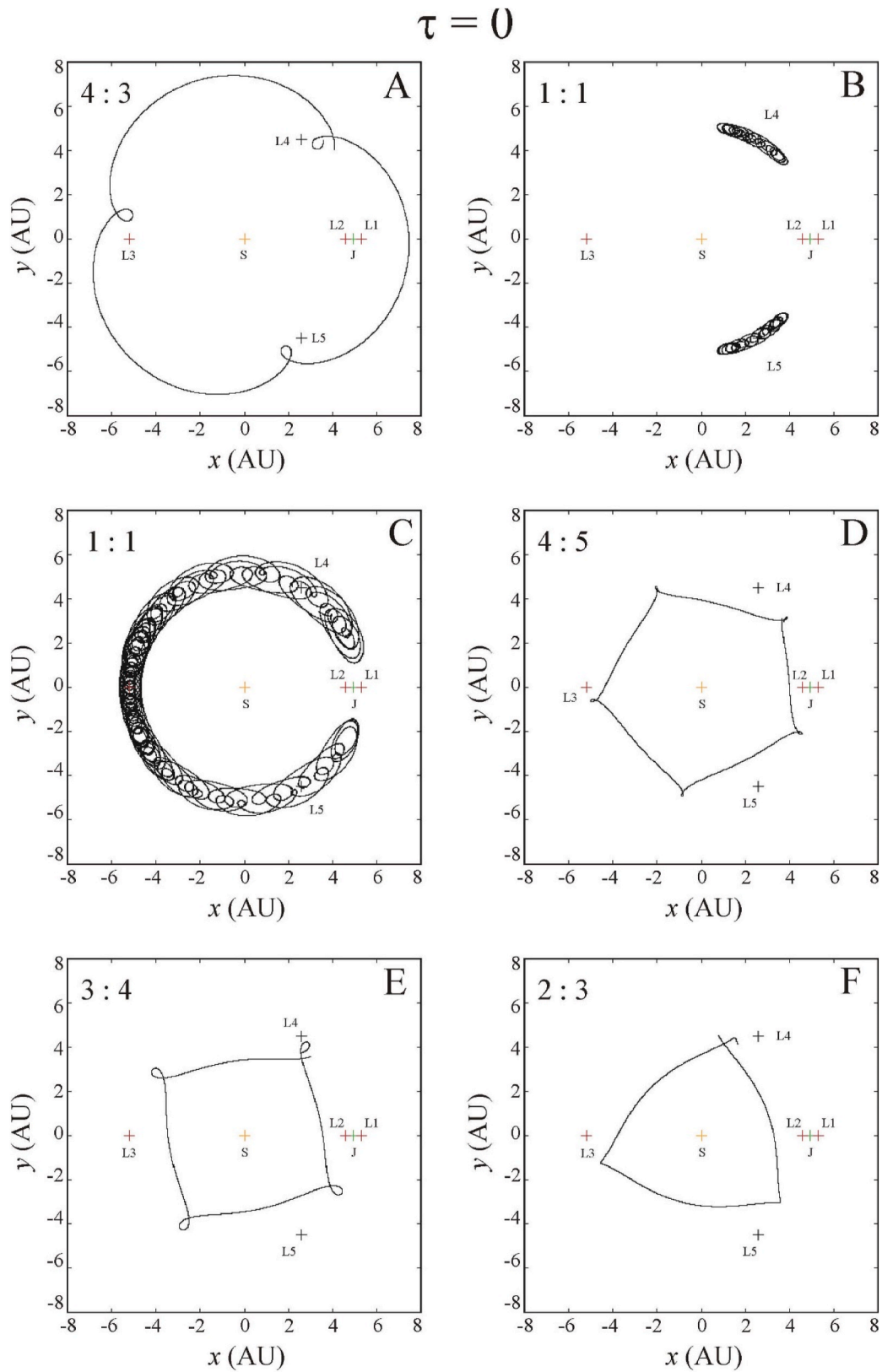


**Fig. 5.** Typical trajectories of particles (asteroids) in 4:3 (A, Supplementary Video Clips VC1, VC7), 1:1 (B, Supplementary Video Clips VC2, VC8, VC9), 1:1 (C, Supplementary Video Clip VC3), 4:5 (D, Supplementary Video Clips VC4, VC10), 3:4 (E, Supplementary Video Clips VC5, VC11), 2:3 (F, Supplementary Video Clips VC6, VC12) first-order resonances with Jupiter. A, D, E, F show 1 revolution, B represents 50 revolutions, and C displays 200 revolutions.

o The asteroid families possessing 4:3, 1:1, 3:4, 2:3, 5:8, 4:7 and 5:9 mean motion resonances with Jupiter may have formed from the asteroids captured, launched and kept on their orbits not only by the stable Lagrange points L4 and L5, but also by the unstable L3 point of the Sun-Jupiter system and certain other areas along the Jupiter's orbit. Jupiter in this way forms a shield which protects the inner Solar System from asteroids moving with speeds not significantly differing from that of Jupiter.

o The asteroid family in 4:5 resonance is captured along the Jupiter's orbit between the L4/L5 points and Jupiter (Fig. 3E and Supplementary Fig. S6E).

o The fact that all the above-mentioned resonant families can be captured from nearby the Jupiter's orbit even simultaneously, suggests their common origin.

o Due to the discontinuos sampling, we can simply determine which regions along Jupiter's orbit are capable to capture asteroids with different resonances.

Our investigations have the following two novelties, none of which has been mentioned in the literature [6,8,14,1,2]: (i) We found two new resonance families of Jupiter, namely the 4:5 and 3:4. (ii) The 4:3, 4:5, 3:4, 2:3 and some higher order resonance families may originate from the Jupiter's orbit. So far, we only knew such an origin about the 1:1 resonance families, the Greeks and Trojans.

Perturbing forces (e.g., the gravitational effect of Saturn and other secular resonances) influence the members of the resonance families. We know that primordial objects of the Hilda group (resonance 2:3) were efficiently removed from their orbits when Jupiter and Saturn crossed their 1:2 mean motion resonance, for instance [6,25] found stable and unstable regions in the 3:2 (Hilda group) and 2:1 (Hecuba group) resonances on the basis of different rates of the chaotic transport (diffusion). They made an interesting prediction for the 4:3 resonance family consisting of only one known member (279 Thule) at the time: since this region is almost as regular as the Hilda group, there must be more than one asteroid there. And indeed, two more asteroids have been found there since then [6].

Presumably, the new resonance families 4:5 and 3:4 detected in our simulations also have stable and unstable regions. Whether it is worthwhile for observers to look for possible members of these two new asteroid families, their stability should be investigated in the future.

## Funding

## Author contributions

Conceptualization: JSB, GH. Data curation: JSB, DH, GH, Formal analysis: JSB, GH. Funding acquisition: JSB, GH. Investigation: JSB, DH, GH. Methodology: JSB, DH, GH. Project administration: JSB. Resources: JSB, GH. Software: JSB, DH. Supervision: GH. Validation: JSB, DH, GH. Visualization: JSB, DH, GH. Writing - original draft: JSB, GH. Writing - review & editing: JSB, GH.

## Declaration of competing interest

The authors declare that they have no known competing financial interests or personal relationships that could have appeared to influence the work reported in this paper.

## Acknowledgements

## Appendix A. Supplementary data

Supplementary data to this article can be found online at https://doi.org/10.1016/j.actaastro.2023.06.005.

## References

[1] K. Tsiganis, H. Varvoglis, J.D. Hadjidemetriou, Stable chaos in the 12:7 mean motion resonance and its relation to the stickiness effect, Icarus 146 (2000) 240–252.

[2] K. Tsiganis, H. Varvoglis, J.D. Hadjidemetriou, Stable chaos high-order Jovian resonances Icarus 155 (2002) 454–474.

[3] K. Tsiganis, H. Varvoglis, R. Dvorak, Chaotic diffusion and effectice stability of Jupiter, Trojans Celestial Mechanics and Dynamical Astronomy 92 (2005) 71–87, https://doi.org/10.1007/s10569-004-3975-7.

[4] R.P. Di Sisto, A. Brunini, L.D. Dirani, R.B. Orellana, Hilda Asteroids Among Jupiter Family Comets Icarus, vol. 174, 2005, pp. 81–89.

[5] M. Cuk, B.J. Gladman, Irregular satellite capture during planetary resonance passage, Icarus 183 (2006) 362–372.

[6] M. Broz, D. Vokrouhlicky, Asteroid Families in the First Order Resonances with Jupiter Monthly Notices of the Royal Astronomical Society, vol. 390, 2008, pp. 715–732, https://doi.org/10.1111/j.1365-2966.2008.13764.

[7] M. Broz, D. Vokrouhlicky, A. Morbidelli, D. Nesvorny, W. F, Bottke Did the Hilda collisional family form during the late heavy bombardment? Mon. Not. Roy. Astron. Soc. 414 (2011) 2716–2727.

[8] B. Érdi, R. Rajnai, Z. Sándor, E. Forgács-Dajka, Stability of higher order resonances in the restricted three-body problem, Celestial Mech. Dyn. Astron. 113 (2012) 95–112.

[9] M.A. Galiazzo, R. Schwarz, Hungaria Region as Possible Source of Trojans and Satellites in the Inner Solar-System Monthly Notices of the Royal Astronomical Society, vol. 445, 2014, pp. 3999–4007.

[10] C. Beaugé, F. Roig, A semianalytical model for the motion of the Trojan asteroids: proper elements and families, Icarus 153 (2001) 391–415.

[11] P. Robutel, F. Gabern, The Resonant Structure of Jupiter's Trojan Asteroids-I. Long-Term Stability and Diffusion Monthly Notices of the Royal Astronomical Society, vol. 372, 2006, pp. 1463–1482, https://doi.org/10.1111/j.1365-2966.2006.11008.

[12] P. Robutel, J. Bodossian, The resonant structure of Jupiter's Trojan asteroids-II, What happens for different configurations of the planetary system Monthly Notices of the Royal Astronomical Society 399 (2009) 69–87, https://doi.org/10.1111/j.1365-2966.2009.15280.

[13] T.A. Michtchenko, C. Beaugé, F. Roig, Planetary migration and the effects of mean motion resonances on Jupiter's Trojan asteroids, Astron. J. 122 (2001) 3485–3491.

[14] F. Marzari, H. Scholl, C. Murray, C. Lagerkvist, Origin and Evolution of Trojan Asteroids Asteroids III, W. F. Bottke Jr., A. Cellino, P. Paolicchi, R. P. Binzel (Eds), University of Arizona Press, Tucson, 2002, pp. 725–738.

[15] F. Marzari, H. Scholl, Dynamics of Jupiter Trojans during the 2:1 Mean Motion Resonance Crossing of Jupiter and Saturn Monthly Notices of the Royal Astronomical Society, vol. 380, 2007, pp. 479–488.

[16] B. Érdi, E. Forgács-Dajka, I. Nagy, R. Rajnai, A parametric study of stability and resonances around L4 in the elliptic restricted three-body problem, Celestial Mech. Dyn. Astron. 104 (2009) 145–158.

[17] R. Rajnai, I. Nagy, B. Érdi, Frequencies and resonances around L4 in the elliptic restricted three-body problem, Mon. Not. Roy. Astron. Soc. 443 (2014) 1988–1998.

[18] R. Schwarz, Á. Bazsó, B. Érdi, B. Funk, Stability and secondary resonances in the spatial restricted three-body problem for small mass ratios, Mon. Not. Roy. Astron. Soc. 443 (2014) 2437–2443.

[19] M. Montesinos, J. Garrido-Deutelmoser, J. Olofsson, C.A. Giuppone, J. Cuadra, A. Bayo, M. Sucerquia, N. Cuello, Dust trapping around Lagrangian points in protoplanetary disks, Astron. Astrophys. 642 (2020), https://doi.org/10.1051/0004-6361/202038758 article A224.

[20] D. Nesvorny, D. Vokrouhlicky, A. Morbidelli, Capture of Trojans by jumping jupiter, Astrophys. J. 768 (2013) 45, https://doi.org/10.1088/0004-637X/768/1/45.

[21] V.J. Srivastava, J. Kumar, B.S. Kushvah, Regularization of circular restricted three-body problem accounting radiation pressure and oblateness, Astrophys. Space Sci. 362 (2017) 49, https://doi.org/10.1007/s10509-017-3021-3.

[22] S. Hellmich, S. Mottola, G. Hahn, E. Kührt, D. de Niem, Influence of the Yarkovsky Force on Jupiter Trojan Asteroids Astronomy & Astrophysics, vol. 630, 2019, p. A148, https://doi.org/10.1051/0004-6361/201834715.

[23] E. Fehlberg, Classical Fifth-, Sixth-, Seventh-, and Eighth-Order Runge-Kutta Formulas with Stepsize Control NASA Technical Report, 1968, p. 287.

[24] V. Szebehely, Theory of Orbits: Appendix I., II, III, Academic Press, New York, 1967, pp. 214–225.

[25] D. Nesvorny, S. Ferraz-Mello, On the asteroidal population of the first-order Jovian resonances, Icarus 130 (1997) 247–258.